Journal of Magnetic Resonance **142,** 74–85 (2000)
Article ID jmre.1999.1917, available online at http://www.idealibrary.com on IDEAL®

Paramagnetic Effects of Iron(III) Species on Nuclear Magnetic Relaxation of Fluid Protons in Porous Media

Traci R. Bryar,[1] Christopher J. Daughney, and Rosemary J. Knight

Department of Earth and Ocean Sciences, University of British Columbia, Vancouver, British Columbia V6T 1Z4, Canada

Received March 25, 1999; revised July 29, 1999

The ^{1}H NMR spin–lattice relaxation time, T_1, of saturated sands depended on the chemistry of the pore fluid, pore size distribution, and relaxivity of the surface. In the absence of paramagnetic impurities, surface relaxivities of quartz sand and silica gel samples of known porosity and surface area at any pH were lower than any previously reported values. Relaxation rate of the bulk pore fluid increased linearly with increasing Fe(III) concentration and varied with speciation of the ion. With only 0.01% of the silica surface sites occupied by sorbed Fe(III) ions, surface relaxivity increased by an order of magnitude. In addition, low concentrations of Fe(III)-bearing solid phases present as surface coatings or as separate mineral grains increased surface relaxation as much as two orders of magnitude. We believe that observations of relatively constant surface relaxivity in rocks by previous researchers were the result of consistently high surface concentrations of paramagnetic materials.

Key Words: **paramagnetic cations; paramagnetic solids; iron(III); porous media; spin relaxation.**

INTRODUCTION

Nuclear magnetic resonance (NMR) has become widely used in the geophysical community in the past ten years. ^{1}H NMR relaxation measurements have been used to estimate a wide variety of petrophysical properties, including porosity, water saturation, pore size distribution, permeability, clay-bound water fraction, and wettability of the solid (*1–7*). Of specific interest in recent hydrogeologic studies has been the use of measured NMR relaxation times to obtain information about pore sizes in rocks and sediments. Field measurements obtained with a surface loop NMR instrument have been used to determine the average pore size in a volume of the subsurface, allowing subsequent classification of the soil as clay, sand, or gravel (*8*). In addition, NMR measurements in the laboratory have been interpreted to determine pore size distribution of aquifer materials (*9*). While it is often assumed that changes in relaxation time correspond to changes in pore size, it is well known that the presence of paramagnetic ions can significantly affect NMR relaxation times (*10*). The presence of paramagnetic materials might therefore introduce significant error into pore size calculations and complicate the comparison of two materials with different paramagnetic content. Although Fe(III) and Mn(II) are generally the most abundant paramagnetic substances in rocks (*11*) and can vary dramatically in concentration and speciation in subsurface materials, there has not been a thorough study of their potential effects on the NMR signal. The objective of our research is to completely characterize the effects of paramagnetic Fe(III) species on NMR of saturated porous materials.

The fact that dissolved paramagnetic ions affect the NMR signal is exploited in borehole NMR logging (*12*) where the addition of paramagnetic ions, such as manganese salts, can be used to reduce the relaxation time of water; this makes it possible to separate the response of the water from that of the hydrocarbon. However, most researchers have assessed the role of dissolved paramagnetic ions in NMR of natural geologic materials to be minimal. For example, Vogeley and Moses (*13*) have concluded that concentrations of aqueous Fe(III) and Mn(II) will be too small to influence NMR measurements due to the low solubilities of most iron- and manganese-bearing minerals.

In a detailed study of the effect of solid paramagnetic species, Foley *et al.* (*14*) manufactured synthetic calcium silicates containing known concentrations of Fe(III) or Mn(II) oxides. They found that relaxation rates for the fluid-saturated porous solids were similar to those observed for natural materials and were proportional to the concentration of paramagnetic ions in the solid. However, the rate only varied by a factor of 5 over the entire range of iron and manganese concentrations tested whereas pore size distributions in natural materials typical vary 4 orders of magnitude. This relatively small paramagnetic effect might explain the apparent insensitivity of NMR measurements to the presence of Fe(III)- and Mn(II)-bearing minerals (*15*), but it is somewhat surprising considering the strong dependence of NMR on dissolved paramagnetic ion concentration.

Another recent study looked at the effect of paramagnetic ions adsorbed to the solid phase. Kenyon and Kolleeny (*16*) found that manganese ions adsorbed to calcite relaxed the system faster than aqueous Mn^{2+}. However, interpretation of

[1] To whom correspondence should be addressed. E-mail: bryar@geop.ubc.ca.

1090-7807/00 $35.00

their experiments involving the adsorption of Fe(II) was complicated by oxidation of some of the iron and precipitation of Fe(III) oxyhydroxide.

The objectives of our research were to investigate and quantify the effect of Fe(III) on the NMR response of geologic materials, taking into account the concentration and chemical form of iron and its location in the rock–water system. Specifically, we measured NMR relaxation rates for water molecules interacting with Fe(III) ions in solution, adsorbed to silica surfaces, precipitated onto the surface, and present in distinct iron-bearing minerals. Our aim is to develop a single model which would predict relaxation parameters for a quartz sand and which would account for varying quantities of Fe(III) in these four states. This will allow for more accurate and meaningful interpretation of NMR data for the characterization of porous materials in both laboratory and field studies.

RELAXATION THEORY IN POROUS MEDIA

For a liquid, the nuclear magnetic relaxation process is coupled with diffusion. If we define $M(\tau)$ as the longitudinal component of ^{1}H nuclear spin magnetization per unit volume at time τ, then M satisfies the diffusion–Bloch equation (*17, 18*),

$$\frac{\partial M}{\partial \tau} = D\nabla^2 M - \frac{M}{T_{1b}}, \qquad [1]$$

where D is the self-diffusion coefficient of the bulk liquid and T_{1b} is the bulk liquid relaxation time constant. When the liquid is confined in a pore, the relaxation time is often found to be much less than T_{1b}. This increased relaxation has been attributed to the presence of relaxation sites on the surface of the solid. ^{1}H nuclear spins in water molecules present in the bulk pore fluid and adsorbed to the surface of the pore relax at different rates, T_{1b}^{-1} and T_{1s}^{-1}, respectively. The two relaxation mechanisms contribute in parallel to the decay,

$$\frac{1}{T_1} = \frac{1}{T_{1b}} + \frac{1}{T_{1s}}. \qquad [2]$$

Adsorbed water molecules exchange with those in the bulk pore fluid. If the exchange is fast enough to maintain uniform magnetization across the pore during decay, that is, if all water molecules interact with the surface during the lifetime of the decay, then the surface relaxation time is proportional to pore size. The observed relaxation rate will be

$$\frac{1}{T_1} = \frac{1}{T_{1b}} + \rho\left(\frac{S}{V}\right)_{\text{pore}}, \quad \text{when } \rho \ll D\left(\frac{S}{V}\right), \qquad [3]$$

where (S/V) is the surface area to volume ratio of the pore and ρ, called the surface relaxivity, is a parameter characterizing the effectiveness of the pore surface relaxation (*17, 18*). Rocks and unconsolidated sands have a distribution of pore sizes, so the observed relaxation of nuclear spin magnetization will be a sum of single-exponential decay terms, one for each uniquely sized pore space experienced by the fluid molecules.

$$M(\tau) = \sum_i m_i \exp(-\tau/T_{i1}), \qquad [4]$$

where each m_i is proportional to the number of ^{1}H nuclear spins relaxing with relaxation time T_{i1}. To effectively calculate pore size distributions for a rock sample from distributions of relaxation times, accurate values for surface relaxivity (ρ) are required.

Our central objective in this study is to account for the role of paramagnetic Fe(III) species in the NMR response. We therefore require a theoretical framework that describes the contributions of paramagnetic species to the measured relaxation rate. The NMR relaxation theory for paramagnetic species in solution was originally developed by Solomon (*19*) and later extended by Bloembergen and Morgan (*20*). For solutions containing paramagnetic ions, the relaxation rate, T_{1b}^{-1}, is a sum of the paramagnetic and diamagnetic contributions,

$$\frac{1}{T_{1b}} = \frac{x}{T_{1M} + \tau_M} + \frac{1}{T_{1W}}, \qquad [5]$$

where x is the mole fraction of water molecules in the hydration shell of the paramagnetic ion, τ_M is the residence time of the water molecules in the hydration shell of the ion, T_{1M} is the relaxation time of a ^{1}H nuclear spin in the hydration shell, and T_{1W} is the relaxation time of pure bulk water. Thus, bulk relaxation rate is proportional to paramagnetic ion concentration as well as the number of water molecules in the hydration sphere of an ion. Experiments with small chelates of Fe^{3+} in water have shown that contributions to relaxation from water molecules outside the first hydration shell are negligible (*21*). The paramagnetic relaxation time (T_{1M}) is determined by the interaction between a ^{1}H nuclear spin on an inner-sphere water molecule and the electron spin (S) of the paramagnetic ion (*22, 23*):

$$\frac{1}{T_{1M}} = \frac{2}{3}\left(\frac{A_s}{\hbar}\right)^2 S(S+1)\left[\frac{\tau_{c2}}{1+(\omega_S\tau_{c2})^2}\right] + \frac{2}{15}\left(\frac{A_d}{\hbar}\right)^2 \times S(S+1)\left[\frac{3\tau_{c1}}{1+(\omega_I\tau_{c1})^2} + \frac{7\tau_{c2}}{1+(\omega_S\tau_{c2})^2}\right]. \qquad [6]$$

S, the spin quantum number, varies with the number of unpaired electrons in the paramagnetic ion ($S = 2.5$ for Fe(III) and Mn(II) but $S = 0.5$ for Cu(II)). τ_{c1} and τ_{c2} are correlation times, which vary with the residence time of water molecules in the hydration sphere, the time constant for molecular rotation, and the time constant for electron spin relaxation caused

by the fluctuation of the spin (S) among its various possible quantum states. ω_I and ω_S are the Larmor frequencies for the nucleus and the electron, respectively. A_s and A_d are the coupling constants for the interactions between the nuclear and electron spins. A_d depends inversely on r^3, where r is the distance between the proton and the center of the paramagnetic ion.

Kleinberg, Kenyon, and Mitra (*22*) further extended the theory to discuss relaxation of fluids at solid surfaces incorporating the ideas of Korringa, Seevers, and Torrey (*23*). They explicitly included the effect of paramagnetic surface sites in their model. The paramagnetic sites can either be surface ions in the crystal lattice, paramagnetic crystal defects, or adsorbed paramagnetic ions. The surface relaxation rate, T_{1S}^{-1}, is given by

$$\frac{1}{T_{1S}} = \frac{x}{T_{1M} + \tau_M} + \frac{1 - x}{T_{1N} + \tau_N}. \quad [7]$$

T_{1N} is the relaxation time of the adsorbed fluid protons not influenced by paramagnetic species and τ_N is the corresponding residence time of water molecules at the surface. In the case of water molecules adsorbed to a paramagnetic-bearing mineral surface, x is the mole fraction of adsorbed water molecules close enough to a paramagnetic site in the solid for the ^1H nuclear spin to couple to the paramagnetic spin, S. This distance is effectively the thickness of one monolayer of water. For paramagnetic ions sorbed to a solid surface, x becomes the mole fraction of adsorbed water molecules within the inner coordination sphere of the ion.

Although Eq. [6], describing the paramagnetic relaxation time, T_{1M}, applies equally to paramagnetic ions in solution and paramagnetic surfaces, the magnitude of some of the parameters differs for the solid and solution cases, and the coupling constants and correlation times change upon adsorption of an ion to a mineral surface. For example, A_d for relaxation at surfaces is different from the solution value because of the anisotropy of restricted rotational motion. A_s varies when bonding in the ion complex changes, affecting the delocalization of the unpaired electrons. If adsorption reduces the number of water molecules in the hydration shell of the ion, the surface relaxation rate, T_{1s}^{-1}, would decrease. For Mn^{2+}, the hydration shell of the adsorbed ion is retained upon sorption to a surface (*24*) but this is not necessarily true for the adsorption of Fe(III) ions. Both the residence time of water molecules in the hydration shell of an Fe(III) ion and correlation times, τ_{c1} and τ_{c2}, for electron spin relaxation can differ by several orders of magnitude for ions in solution and on a surface.

METHODS AND MATERIALS

Materials and NMR Sample Preparation

Silica gel (60 Å, 70–230 mesh, BDH Inc.) and quartz sand (99.995%, >40 mesh, silicon(IV) dioxide, Aesar) were used in this study as analogs for naturally occurring mineral surfaces. Both materials were rinsed repeatedly with 10% HCl and distilled, deionized (DDI) water (18 MΩ cm) to remove paramagnetic impurities. Surface areas were measured by the Brunauer–Emmett–Teller (BET) N_2 adsorption method and grain densities were measured with a helium pycnometer. The properties of these materials are listed in Table 1.

TABLE 1
Properties of Materials Used in This Study

Property	Silica gel	Quartz sand	Pseudobrookite
Grain size distribution	70–230 mesh	50–200 mesh	<100 mesh
Surface area ($m^2\ g^{-1}$)	356	0.20	0.1
Grain density ($g\ cm^{-3}$)	2.1	2.65	4.36
Porosity	0.77	0.45	Not applicable
Surface area to pore volume ratio (μm^{-1})	223	0.65	Not applicable

Saturated solid samples for NMR were prepared by mixing 10.0 g of solid with 50.0 mL of 0.01 M NaCl electrolyte in acid-washed Nalgene plastic bottles. pH was adjusted with reagent grade HCl or NaOH solutions and the mixtures were equilibrated for 3 days at 25.0°C in a tumbler. After equilibration, excess pore fluid was removed and filtered using 0.45 μm, hydrophilic polyether sulfone filters (Gelman, Supor Acro disk). Filtered solutions were analyzed for metals by inductively coupled plasma atomic emission spectroscopy (ICP-AES, Analytical Service Laboratories Ltd., Vancouver, Canada). Representative, 1 mL samples of the saturated solid were transferred to 10 mm o.d. NMR tubes (Wilmad Glass) and centrifuged for 5 min to ensure uniform packing and consistent porosity. All excess pore fluid was removed from the surface of the sample before NMR data were collected. The NMR tube lids were sealed with Parafilm to minimize water loss. Measurements of the relaxation time of the bulk pore fluids (T_{1b}) were made using approximately 0.5 mL of the filtered, equilibrated pore fluid in an NMR tube. The method described above was necessary to ensure an adequate quantity of equilibrated pore fluid for chemical tests and T_{1b} determination. The process required that NMR samples not be degassed or weighed before and after saturation. Consequently, the pore fluid contained dissolved oxygen, and porosity could not be obtained from integrals of the T_1 distribution peak amplitudes. Porosity was measured independently using representative samples.

Paramagnetic solutions were prepared in DDI water using $Fe(NO_3)_3 \cdot 9H_2O$. NMR measurements were carried out on bulk Fe(III) solutions at pH ~2.5 for concentrations from 0.0 to 10.0 mg Fe L^{-1}. To investigate variation of T_{1b} with pH, solutions from 0.0 to 5.0 mg Fe L^{-1} were prepared at pH 1.0, from 0.0 to 2.8 mg Fe L^{-1} at pH 2.0, and from 0.0 to 0.5 mg Fe L^{-1} at pH 3.0.

To assess the influence of paramagnetic Fe(III) ions adsorbed to sand surfaces, quartz sand was equilibrated with acidic, dilute (0.50 mg Fe L^{-1}) solutions of Fe(III). pH was varied from 1.0 to 3.2 to control the fraction of ions adsorbed to the solid. The adsorption experiment was repeated with silica gel equilibrated with 5.0 mg Fe L^{-1} solutions of Fe(III), taking advantage of the gel's high surface area to increase the amount of iron sorbed to the surface. The extent of iron sorption was determined by the disappearance of Fe from solution. Solutions were filtered, acidified, and analyzed by flame atomic absorption spectroscopy (FAA). Although the pH of pore fluids in natural settings will not be as low as those used in this experiment, we used acidic solutions to avoid precipitation of solid phases, which would complicate interpretation of the results.

The paramagnetic mineral selected for this study was pseudobrookite (Fe_2TiO_5, <100 mesh, Sigma), because it was available in pure form with a grain size distribution similar to that of the silica gel (Table 1). Saturated homogeneous mixtures of silica gel and Fe_2TiO_5 (from 0.5 to 25% by weight) were prepared to assess the influence of paramagnetic minerals on NMR relaxation. The porosities of the silica gel–pseudobrookite mixtures were the same (within 1%) as that of silica gel. The pH of the pore fluid was kept between 5.5 and 5.7 to minimize solubility of the mineral. In this pH range, dissolved iron concentrations are less than 10^{-7} M.

To evaluate the influence of iron(III) oxyhydroxide coatings, eight silica gel samples and two quartz sand samples with different amounts of iron(III) oxyhydroxide coatings were prepared by the method of Grantham *et al.* (*25*). Mixtures of aqueous $FeSO_4$ and sand or gel were oxidized by the addition of excess 30% H_2O_2 and left standing overnight. The iron oxyhydroxide-coated solids were then rinsed with DDI water and dried. Within experimental error, neither the porosity nor the surface area of the solids was affected by the coatings. The distribution of the iron on the coated surface was investigated qualitatively by energy-dispersion spectrometry (EDS) using a Philips XL-30 scanning electron microscope (SEM). The oxyhydroxide precipitate did not always form a uniform coating. Thus, not all of the precipitated Fe(III) atoms are necessarily surface atoms, because they may be buried beneath other molecules of Fe(III) oxyhydroxide. The amount of iron on each gel and sand sample (mg of Fe g^{-1} of solid) was determined by leaching the iron from a representative subsample of the solid with 10% HCl and determining iron concentration by FAA.

NMR Experiments

Relaxation data were collected using a 90 MHz ^{1}H NMR spectrometer (Bruker) with a 2.2 T iron-core electromagnet and an SXP probe (10 μs dead time). A modified inversion–recovery pulse program was used, in which the free induction decay (FID) from a [180°–τ–90°] pulse sequence is subtracted from the FID from a 90° pulse (equivalent to a measurement at infinite τ). This pulse sequence has the advantage that it is less sensitive to imperfections in the 180° pulse. It always gives zero amplitude as τ approaches infinity,

$$M(\tau) = M_0 \exp(-\tau/T_1), \qquad [8]$$

and thus can be fitted with only two parameters (M_0 and T_1). The original inversion–recovery experiment requires a three-parameter fit (M_0, ϵ, T_1) because imperfect 180° pulses give the dependency

$$M(\tau) = M_0[1 - \epsilon\ 2\ \exp(-\tau/T_{i1})], \qquad [9]$$

where $\epsilon < 1$. Data for each sample were collected at room temperature, with 30 randomly sequenced, exponentially spaced (from 0.5 ms to 12 s), delay times (τ) summed 24 times. The wait time between scans was 15 s. There were no evaporative losses of water from the sample during data collection. Both intensity and standard deviation of the intensity were recorded for each τ; the signal-to-noise ratio of the data was always greater than 300.

The multiexponential decay of magnetization (Eq. [4]) was fit to a distribution of 160 exponentially spaced T_1 values (ranging from 1 ms to 10 s) using regularized nonnegative least-squares and least-distance inversion routines (*26, 27*). Since this approach does not assume any particular model, it gives a less biased interpretation of the data than a single-exponential, stretched-exponential, or double-exponential fit. Ideally, to avoid artifacts resulting from inversion, the solution space should be continuous with width (1 ms to 10 s) less than the range of data collected (0.5 ms to 12 s). We limited the T_1 distribution to 160 points to keep processing time down. The regularized relaxation time distributions were calculated with Relax-NMR (Frank Linseisen, University of British Columbia, Department of Physics, Vancouver, Canada; personal communication, 1998). Inversion parameters were selected so that each datum was misfit by approximately one standard deviation. For convenience in comparison of data, the reported T_1 value for a measurement is the geometric mean of the distribution. Uncertainties in T_1 were obtained by repeat measurements. In the case of a monomodal distribution, the geometric mean T_1 is equal (within experimental error) to the T_1 value obtained from a fit to a single-exponential decay if the distribution is sufficiently narrow. Surface relaxivity values were calculated using Eq. [3] with the substitution

$$\left(\frac{S}{V}\right)_{\text{pore}} = \frac{1-\phi}{\phi}\left(\frac{S}{V}\right)_{\text{grain}} = \frac{1-\phi}{\phi}\left(\frac{S}{m}\right)_{\text{g}} \rho_{\text{g}}, \qquad [10]$$

where ϕ is porosity, (S/m) is the surface area to mass of the grains ($m^2\ g^{-1}$) obtained from BET N_2 adsorption, and ρ_g is the grain density.

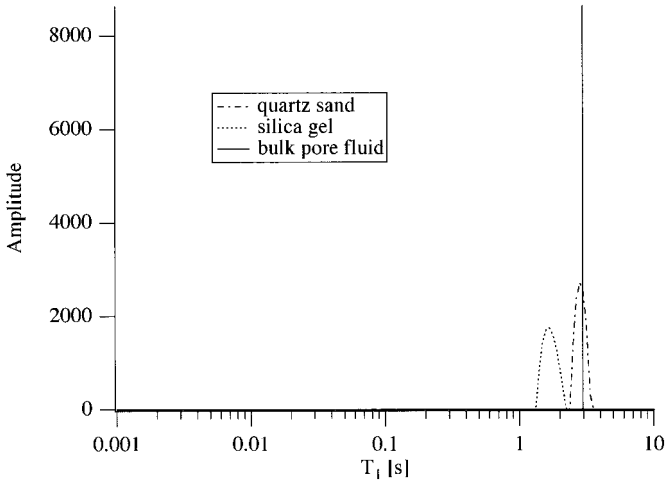

FIG. 1. NMR spin–lattice relaxation time (T_1) distribution of extracted pore fluid, saturated pure quartz sand, and saturated silica gel at pH 5. The amplitudes have not been normalized to water content to indicate porosity.

RESULTS AND DISCUSSION

NMR of Saturated Pure Quartz Sand and Silica Gel

The first set of measurements was made on the sand and silica gel samples saturated with 0.01 M NaCl solutions with pH varying from 1 to 8. NMR measurements were made on the extracted pore fluids (after equilibration with the solids) and on the saturated porous samples. The relaxation time determined for the pore fluid and the relaxation distributions for the water-saturated silica gel and sand at pH 5 are shown in Fig. 1. The form of these data is typical of all the measurements in this first set of experiments. The amplitude on this plot is a measure of the amount of water relaxing with each relaxation time T_{1i}, but the fact that the three distributions in Fig. 1 have different amplitudes simply means that the mass of each sample was different. The amplitude can be normalized to give an indication of total water-filled porosity, but we have not done so in this study. The bulk pore fluids, extracted from the saturated sand and gel samples, were always found to have a single relaxation time, indicating that all water molecules in the electrolyte relax at the same rate. In contrast, the distributions for the silica gel and the sand were both found to be monomodal, with the distribution for the gel slightly broader than that for the sand; this is due to the gel's broader distribution of pore size. It is interesting to note that the microporosity of the gels does not produce a separate peak with low T_1. The relaxation is slow enough to allow diffusion of the water molecules between micropores and macropores; thus the T_1 distribution reflects the average pore size distribution (*28*).

The relaxation times for extracted pore fluid, saturated silica gels (11 samples), and quartz sands (17 samples) showed no dependence on pH for either the bulk fluids or the saturated solids. We conclude that protonation of surface-bound water molecules has no direct effect on T_1 or ρ. Our results suggest that the increase in surface relaxivity at low pH observed for natural sand (*29*) cannot be explained by the protonation of adsorbed water molecules alone.

The relaxation time T_{1b} of the bulk fluids was found to be equal to 2.88 $\pm$ 0.04 s. This value is less than the relaxation time of 3.3 s that has been determined for pure water at this temperature and magnetic field (*30*) and is due to the presence of dissolved O_2 (*31*). The presence of oxygen in the samples was required to stabilize the iron in the desired +3 oxidation state. The oxygen did not affect the already oxidized surface minerals nor did it interfere with ion–surface interactions. The oxygen was evenly distributed throughout the unconsolidated samples used in this study. If rock cores had been used in place of sand, some pores could have remained anoxic even when the sample was saturated with oxygenated fluid.

The relaxation time for the saturated silica gel is 1.64 $\pm$ 0.09 s, significantly lower than that of the bulk pore fluids due to the high surface area of this material. Surface relaxivity (ρ) of the silica gel, calculated using Eq. [3], was (1.2 $\pm$ 0.2) $\times$ 10^{-3} μm s^{-1}, slightly lower than relaxivities reported by previous researchers (Table 2) for similar materials.

The relaxation time for the saturated sand is 2.81 $\pm$ 0.05 s, very close to the T_{1b} of the bulk fluid, and the highest T_1 value ever reported in the literature for a water-wet mineral surface. Surface relaxivity (ρ) of the sand, calculated from the measured T_1 and T_{1b} values using Eq. [3], was found to be zero within experimental error (0.013 $\pm$ 0.015 μm s^{-1}). This is at least an order of magnitude lower than any previously reported value for silica sand or sandstone (Table 2). For example, the relaxivity reported for pure quartz grains used in (*16*) was 0.83 μm s^{-1}, the residual relaxivity of synthetic calcium silicates with no added paramagnetic ions was 0.406–4.04 μm s^{-1} (*14*), and silica sand had surface relaxivity ranging from 2.89 to 3.06 μm s^{-1} (*9*). We believe that we have obtained this low value of surface relaxivity for our quartz sand because of the purity of the quartz that we have used and suggest that the higher values reported in the literature result from trace impurities of paramagnetic minerals in the samples. The implication of these results is that variations in surface relaxivity are potentially as

TABLE 2
Surface Relaxivity Parameter for Porous Materials

Material	Surface relaxivity, ρ (μm s^{-1})	Reference
Silica gel	1.2×10^{-3}	This work
Porous silica glass	1.8×10^{-3}	(*37*)
Silica gel	4.2×10^{-3}	(*38*)
Silica gel	(3.1–7.7) $\times$ 10^{-3}	(*9*)
Quartz sand	0.0 (i.e., 0.013 $\pm$ 0.015)	This work
Quartz	0.83	(*16*)
Synthetic Ca silicate	0.406–4.04	(*14*)
Silica sand	2.89–3.06	(*9*)
Sandstone rocks	9.0–46	(*34*)

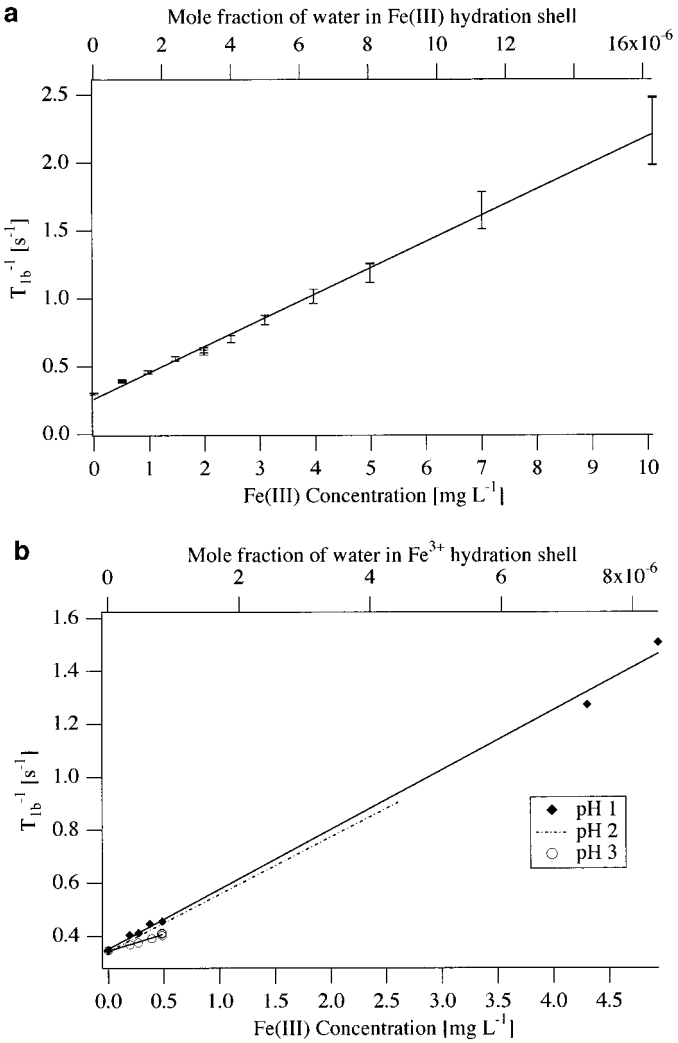

FIG. 2. Dependence of relaxation rate of bulk solutions on Fe(III) ion concentration: (a) at pH roughly 2.5; (b) at pH 1.0, 2.0, and 3.0. To improve legibility of (b), data points for pH 2.0 are not shown; the linear fit is given in their place.

significant as variations in pore size; both properties can vary by several orders of magnitude, so observed differences in relaxation time cannot necessarily be attributed to differences in pore size.

NMR of Fe(III) Ions in Solution

NMR measurements on iron solutions were carried out to explore the relationship between relaxation time and Fe(III) ion concentration as well as the influence of ion speciation on T_1. Relaxation time distributions calculated from the NMR measurements consisted of a single discrete relaxation time, as expected for solutions. The relaxation rate increased linearly with concentration of Fe(III) at pH ~2.5 (Fig. 2a). The scatter in the data was the result of small variations in pH. The time $\tau_M + T_{1M}$ (residence time of water molecules in the inner coordination sphere of Fe(III) plus the relaxation time of proton nuclear spins in those water molecules), calculated from the slope of Fig. 2a using Eq. [5], was approximately 10 μs. For NMR of saturated sandstones, there is some precedent for setting $\tau_M + T_{1M} \approx T_{1M}$ (*22, 32*). However, Bertini *et al.* (*33*) have shown that τ_M can be almost as large as T_{1M} for aqueous solutions of Fe^{3+} at room temperature. Because this ambiguity cannot be resolved without measurements at different temperatures, we will discuss variations in the sum $\tau_M + T_{1M}$ rather than variations in T_{1M}.

T_{1b} of solutions cannot be predicted entirely on the basis of total dissolved Fe concentration because relaxation rates of Fe(III) solutions are sensitive to pH-dependent speciation of the ion. For solutions of the same iron concentration, T_{1b} decreased with pH (Fig. 2b). For example, relaxation time of a 0.5 mg Fe L^{-1} solution was 0.3 s lower at pH 1 than at pH 3. At pH 1, Fe(III) is present mostly as $[Fe(H_2O)_6]^{3+}$, but at pH 3 hydrolysis reactions change the iron to a mixture of $[Fe(H_2O)_6]^{3+}$, $[Fe(H_2O)_5OH]^{2+}$, and $[Fe(H_2O)_4(OH)_2]^{+}$. Although all species contain Fe(III), the number of exchangeable water molecules in the hydration sphere decreases as pH increases, decreasing relaxation rate.

When differences in iron speciation are taken into account, $\tau_M + T_{1M}$ can be calculated for each of the three iron complexes from the slopes of the three lines in Fig. 2b using Eq. [5] by assuming that the observed $\tau_M + T_{1M}$ is a weighted average of each complex's $\tau_M + T_{1M}$. These values are shown in Table 3 along with representative values from the literature. $\tau_M + T_{1M}$ for $[Fe(H_2O)_6]^{3+}$ and $[Fe(H_2O)_5OH]^{2+}$ were the same (8 μs) within experimental error, approximately twice that of a previously reported value for $[Fe(H_2O)_6]^{3+}$ (*33*). $\tau_M + T_{1M}$ for $[Fe(H_2O)_4(OH)_2]^{+}$ was 26 μs, approximately triple that of

TABLE 3
Surface Relaxivity Parameter and Relaxation Rate for a Variety of Iron(III) Materials at 25°C

Material	Surface relaxivity, ρ_{Fe} (μm s^{-1})	$\tau_M + T_{1M}$ (μs)
$[Fe(H_2O)_6]^{3+}$	—	8.4 ± 1.0
$[Fe(H_2O)_6]^{3+}$	—	3.6[a]
$[Fe(H_2O)_5OH]^{2+}$	—	8.3 ± 0.9
$[Fe(H_2O)_4(OH)_2]^{+}$	—	26 ± 3
$[Mn(H_2O)_6]^{2+}$	—	6.7[b]
Fe(III) adsorbed to silica	100–160[c]	3.0–1.9[c]
Mn(II) adsorbed to silica	0.7[b]	450[b]
Fe_2TiO_5	130 ± 30	2.3 ± 0.5
Fe(III) oxyhydroxide	10–120[d]	2.5–30[d]

[a] Bertini *et al.* (*33*).
[b] Experiments at 4°C. ρ_{Mn} and $\tau_M + T_{1M}$ calculated from data in Roose *et al.* (*24*).
[c] The range depends on the number of water molecules in the coordination sphere of each adsorbed Fe(III) ion.
[d] The large range of possible values results from the wide scatter of the data shown in Fig. 8.

$[Fe(H_2O)_6]^{3+}$. Either the four inner-sphere water molecules are more tightly bound in $[Fe(H_2O)_4(OH)_2]^{+}$ or changes in delocalization of the unpaired electrons have occurred, affecting relaxation of the electron spin or the coupling between the nuclear and electron spins. For comparison, $\tau_M + T_{1M}$ for $[Mn(H_2O)_6]^{2+}$ measured at 4°C was 6.7 μs (*24*), very similar to the values for $[Fe(H_2O)_6]^{3+}$ reported in Table 3. This similarity may be the result of similar T_{1M} and τ_M values, implying that the residence time of water molecules within the coordination sphere of the ions (τ_M) does not vary significantly with temperature for dissolved ions. Alternatively, a higher τ_M at 4°C may be offset by a slightly lower T_{1M} for $[Mn(H_2O)_6]^{2+}$ than for $[Fe(H_2O)_6]^{3+}$.

Sorption of Fe(III) Ions

To study the effect of sorbed Fe(III) ions on the NMR response of saturated porous solids, we saturated the sand and gel with a solution containing a known concentration of Fe(III) and varied the pH. At the lowest pH, Fe(III) ions will stay in solution, but with increasing pH, the Fe(III) ions leave the solution and adsorb to the solid. Concentrations of adsorbed Fe(III) ions as low as 0.5 μg of Fe g^{-1} of quartz were found to influence the NMR response.

When quartz sand was equilibrated with a 0.50 mg L^{-1} Fe(III) solution, chemical analysis of the pore fluid after equilibration showed that no adsorption of Fe(III) ions occurred at pH 1; that is, all Fe(III) remained in solution. When the chemical analysis was repeated at pH 2.1, it was impossible to determine if any iron adsorbed to the quartz within experimental error. Measurements at pH 3 showed that only 0.40 ± 0.05 mg L^{-1} Fe(III) remained in solution; roughly 20% (±10%) of the iron adsorbed to the quartz sand.

The measured relaxation times of the equilibrated pore fluids and of the fluid-saturated quartz sand samples as pH was varied are shown in Fig. 3a. At pH 1, T_1 of the saturated sand was approximately equal to the relaxation time of the pore fluid, indicating that surface relaxation (T_{1S}^{-1}) was insignificant. This confirmed that negligible surface relaxation takes place in the absence of surface paramagnetic ions. At pH 3, T_{1b} of the pore fluid has increased 15% relative to T_{1b} at pH 1. If dissolved and adsorbed Fe(III) ions were equally efficient relaxing agents, we would expect to see T_{1b} increase as iron was lost from solution and T_1 of the saturated sand remain constant (total concentration of iron in the sample remains constant). The trend in Fig. 3a indicates that this is not the case. At pH 3, T_1 of the saturated sand with 0.5 ± 0.3 μg of Fe g^{-1} of sand adsorbed to the surface was 23% lower than at pH 1. Fe(III) ions adsorbed to the surface relaxed the water molecule ^1H nuclear spins more effectively than dissolved Fe(III) ions. Surface relaxivity of the quartz sand calculated from the data using Eq. [3] increased from 0.01 to 0.3 μm s^{-1} as surface iron concentration increased from 0.0 to 0.5 ± 0.3 μg of Fe g^{-1} of sand. This corresponds to an order of magnitude increase in ρ with only 0.5% (±0.3%) of the sand surface sites occupied by Fe(III) ions.

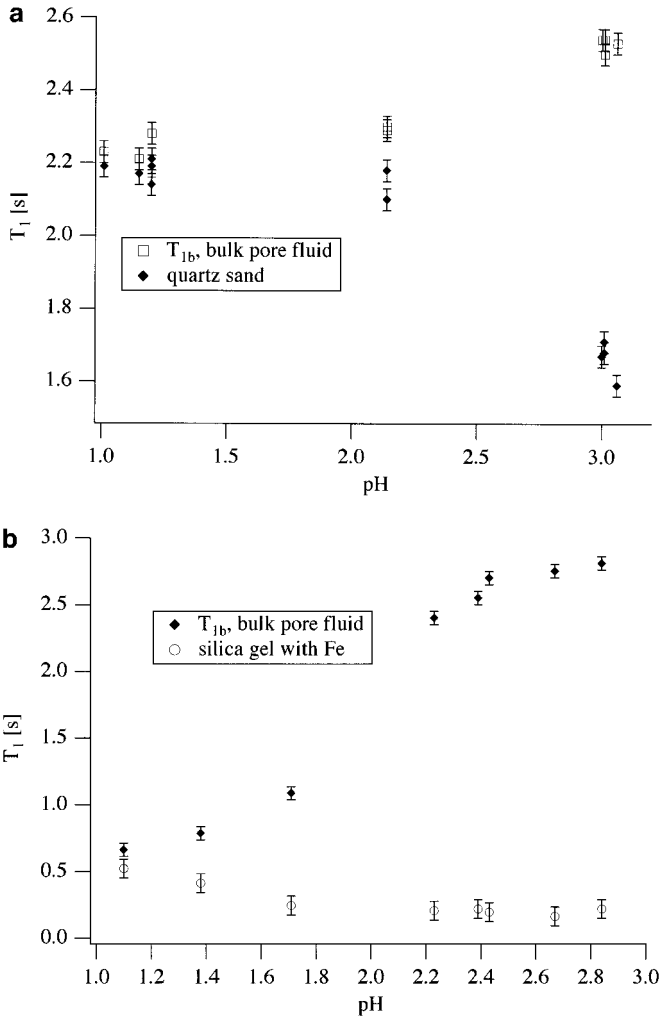

FIG. 3. Dependence of T_1 relaxation time on pH (a) for pure quartz sand equilibrated with 0.5 mg L^{-1} Fe(III) solution and (b) for silica gel equilibrated with 5.0 mg L^{-1} Fe(III) solutions.

When the Fe adsorption experiment was repeated with silica gel, the higher surface area allowed us to use higher concentrations of Fe(III), subsequently improving the precision of iron concentration measurements. Figure 4 shows the relationship between pH and Fe(III) surface concentration on silica gel. The amount of sorbed iron increased from 0.0 to 22 μg of Fe g^{-1} of silica (1.1×10^{-9} mol of Fe m^{-2}) as solution pH increased from 1 to 3.

The measured relaxation times of the equilibrated pore fluids and of the fluid-saturated silica gel samples as pH was varied are shown in Fig. 3b. The same trends observed for quartz sand in Fig. 3a can be seen in Fig. 3b for silica gel. T_1 of the saturated silica gel was approximately equal to the relaxation time of the pore fluid at pH 1 because surface relaxation was negligible with no iron adsorbed to the solid. T_{1b} of the pore

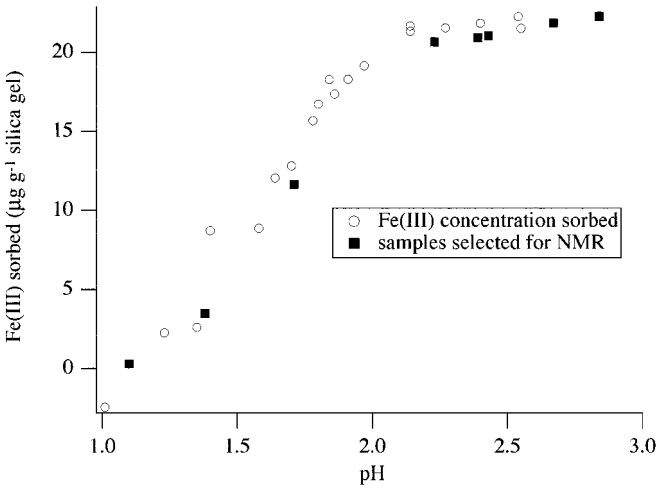

FIG. 4. Concentration of Fe(III) ions sorbed as a function of pH for silica gel equilibrated with 5.0 mg L^{-1} Fe(III) solution. NMR relaxation data (see Fig. 3b) were collected for the samples shown as solid squares.

fluid increased as Fe(III) ions were removed from solution, adsorbing to the surface, and T_1 of the saturated gel decreased as the surface concentration of iron increased. These results confirm that the presence of paramagnetic ions on the surface significantly affects surface relaxation (T_{1S}^{-1}) and that adsorbed Fe(III) is a better relaxing agent than dissolved Fe(III). This phenomenon can be explained by restricted rotational motion of adsorbed species resulting in a longer rotational correlation time for the coordinated water molecules.

Calculated surface relaxivity values for silica gel as a function of the surface concentration of sorbed Fe(III) are shown in Fig. 5. With the relationship between pH and adsorbed Fe(III) firmly established by Fig. 4, we were able to plot ρ with respect to Fe(III) surface concentration rather than pH. The surface relaxivity increased linearly from 0.0012 to 0.020 μm s^{-1} as the surface concentration of iron increased to 21 μg of Fe g^{-1} of silica (1.0×10^{-9} mol of Fe m^{-2}), an order of magnitude increase when only 0.012% of the silica surface sites were occupied by Fe(III) ions. In comparison, surface relaxivity of 4.09 μm s^{-1} resulted from the adsorption of 0.019 mol of Mn(II) ions per m^2 (*16*). If we make the assumption that the linear relationship in Fig. 5 can be extended to higher surface Fe concentrations, our results suggest that Fe(III) adsorbed to quartz or amorphous silica is thousands of times more efficient a relaxing agent than Mn(II) adsorbed to calcite. Obviously, rotational correlation times are affected by adsorption differently depending on the metal and the type of surface involved.

The fact that surface relaxivity increases with surface concentration of Fe(III) suggests that an adsorbed Fe(III) ion has an inherent surface relaxivity for its coordinated water molecules in the same way that dissolved Fe(III) ions have their own unique $\tau_M + T_{1M}$.

Solid Iron(III) Phases

To study the effect of Fe(III) minerals on the NMR response of saturated porous solids, we measured T_1 of saturated mixtures of Fe_2TiO_5 grains (pseudobrookite) and silica gel. Water molecule ^1H nuclear spins can relax by adsorbing to silica gel or to psuedobrookite surfaces; by varying the weight percent of pseudobrookite in the mixtures, we were able to change the fraction of Fe(III)-containing solid surface exposed to the pore fluid. Although the mixtures contained as much as 25% Fe_2TiO_5 by weight, neither the porosity nor the pore size distribution was altered significantly; this was because of the large disparity in surface area (0.1:356 m^2 g^{-1}) and density (4.36:2.1 g cm^{-3}) for the two materials. At 25% pseudobrookite concentration, the fraction of exposed surface as Fe_2TiO_5 was only 0.01% of the total surface area.

Relaxation time distributions for saturated mixtures were monomodal, like that of the pure silica gel relaxation distribution shown in Fig. 1. The T_1 distributions for mixtures containing more than 15% Fe_2TiO_5 by weight were slightly broader than those with less pseudobrookite. The relaxation time of the bulk pore fluid (T_{1b}) for each sample was 2.82 $\pm$ 0.05 s, indicating that negligible quantities of Fe(III) dissolved from Fe_2TiO_5.

Surface relaxivity, calculated from T_1 and T_{1b} using Eq. [3], is shown in Fig. 6 along with the surface relaxivity of pure silica gel for comparison. ρ increased linearly from 0.0012 to 0.015 μm s^{-1} as the Fe(III)-bearing mineral increased from 0 to 25% by weight (0.01% of the total surface area). We believe that each mineral present (silica and pseudobrookite) has its own unique surface relaxivity and the observed relaxivity for the mixtures is a weighted average of those specific surface relaxivities. It is also likely that the direct proportionality is conserved at much higher relaxivities than 0.015 μm s^{-1}; Foley

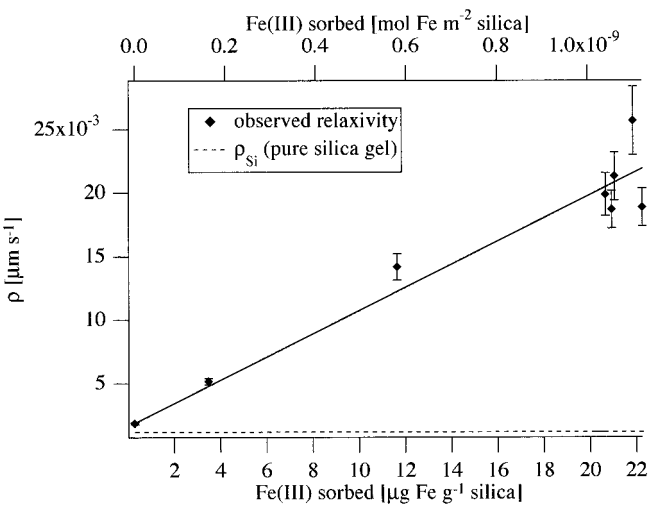

FIG. 5. Dependence of surface relaxivity on concentration of sorbed Fe(III) ions for silica gel equilibrated with 5.0 mg L^{-1} Fe^{3+} solutions. The surface relaxivity for pure silica gel is shown as a dashed line for comparison.

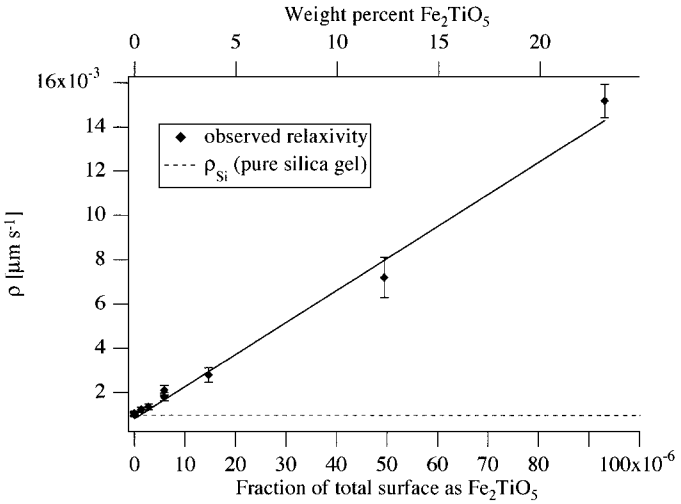

FIG. 6. Dependence of surface relaxivity on weight percent of pseudobrookite (Fe_2TiO_5) and fraction of total surface area as Fe_2TiO_5 in mixtures of silica gel and pseudobrookite at pH 5.5–5.8. The surface relaxivity for pure silica gel is shown as a dashed line for comparison.

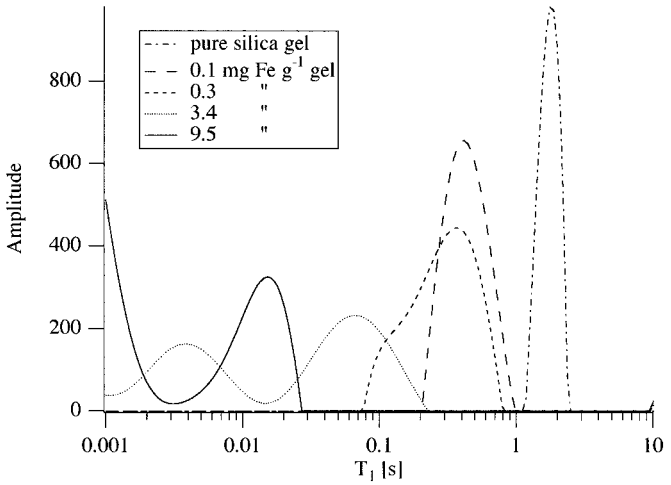

FIG. 7. Regularized NMR spin–lattice relaxation time (T_1) distributions for saturated silica gel with different surface concentrations of amorphous iron oxyhydroxide.

et al. (*14*) have shown that the relationship between concentration of Fe(III) mineral and ρ remains linear for relaxivities as high as 10 μm s^{-1}. As the exposed surface occupied by Fe_2TiO_5 approaches 100%, the linear relationship in Fig. 6 may begin to plateau. This will happen if all of the adsorbed water molecules can be relaxed by an Fe(III) site when the Fe(III)-bearing mineral occupies less than 100% of the surface area. We conclude that, at least in this case, NMR relaxation measurements were very sensitive to the presence of a paramagnetic solid phase.

In naturally occurring sands and sandstones, precipitated iron oxides are commonly present as surface coatings on the silica grains (*11*). To determine the influence of small concentrations of Fe(III) oxide impurities coating the surfaces of porous solids on NMR, we prepared quartz sand and silica gel samples with varying surface concentrations of Fe(III) oxyhydroxide. T_1 distributions for a few of the saturated Fe(III)-coated silica gel samples are shown Fig. 7. The amplitude on this plot is a measure of the amount of water relaxing with each relaxation time T_{1i}, but the fact that the distributions in Fig. 7 have different amplitudes simply means that the mass of each sample was different. T_1 distributions for the Fe(III)-coated sands (not shown) were monomodal, but distributions for coated silica gels changed from monomodal to bimodal as the concentration of iron on the solid surface increased. The bimodal distributions indicate that the microporosity of the silica gel can be distinguished from its macroporosity when concentrations of iron are 0.3 mg g^{-1} or more. An increase in surface relaxivity has shortened the time scale of the relaxation process enough that the water molecules do not have time to diffuse between the micropores and macropores (*28*).

Surface relaxivities calculated using T_{1b} and geometric mean T_1 values for Fe(III) oxyhydroxide coated silica gel and quartz sands are shown in Fig. 8. The data are widely scattered as a result of the difficulty in determining the surface concentration of Fe(III); the pattern of precipitation was such that some Fe(III) is buried under other molecules of Fe(III) oxyhydroxide. In general, surface relaxivities vary by at least two orders of magnitude over the range of concentrations tested. The relaxivity for quartz sand with 2×10^{-5} mol of Fe m^{-2} (0.64 μm s^{-1}) is similar to ρ observed for silicate materials with low levels of paramagnetic impurities (*16*) (Table 2). Sand and sandstone samples typically have relaxivity values which range from 5 to 50 μm s^{-1} (*9, 34*). Our results indicate that a relaxivity parameter of 50 μm s^{-1} would require between 10^{-3} and 10^{-2} mol of Fe(III) m^{-2} surface, a reasonable surface concentration of Fe(III) oxyhydroxide for a high iron content sandstone.

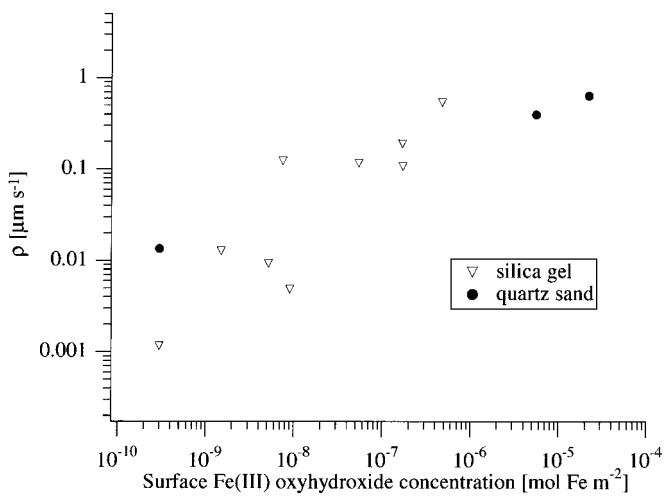

FIG. 8. Dependence of surface relaxivity on surface concentration of amorphous iron oxyhydroxide precipitated on silica gel and quartz sand.

SURFACE RELAXIVITY OF IRON(III)

Surface relaxivity values measured using the well-characterized model systems in this study increased with iron content (μg of Fe g^{-1} of solid); however, this increase was not the same for adsorbed Fe(III) ions, Fe(III)-containing mineral grains, or Fe(III) oxyhydroxide coatings. Instead, relaxivity increased with the fraction of solid surface containing Fe sites. From Eqs. [3] and [7] the surface relaxation rate is

$$\frac{1}{T_{1S}} = \rho\left(\frac{S}{V}\right)_{pore} = \sum_i \frac{x_i}{(T_{1M} + \tau_M)_i}, \quad [11]$$

implying that surface relaxivity should depend on the fraction of water molecules coordinated to a paramagnetic iron atom (x_i) and that there is an inherent relaxivity, ρ_i, for each of the "types" of solid surface represented in Eq. [11]:

$$\rho = \sum_i n_i \rho_i. \quad [12]$$

The coordinated fraction of water molecules, x_i, is related to n_i, the fraction of total surface, by

$$x_i = \frac{n_i h S}{V_{pore}}, \quad [13]$$

where h is the thickness of one monolayer of water, so

$$\rho_i = \frac{h}{(T_{1M} + \tau_M)_i}. \quad [14]$$

If a pure surface or a paramagnetic site on a surface is considered to have its own inherent surface relaxivity value (ρ_i) that is constant, then the surface relaxivity for adsorbed Fe(III) ions and for Fe(III) in different solid phases can be calculated using Eqs. [12]–[14]. These calculated values are shown in the lower half of Table 3 along with the literature values for adsorbed Mn(II).

Accurate calculation of ρ_{Fe} or $(\tau_M + T_{1M})_{Fe}$ for adsorbed ions requires some knowledge of the structure of the hydration shell of an adsorbed ion. Schindler *et al.* (*35*) suggested that ion adsorption occurs through the formation of a surface complex involving deprotonated silanol groups as ligands and loss of one or two coordinated water molecules from the ion's hydration shell. In contrast, adsorption isotherms of several polyvalent cations showed that the inner coordination sphere of hydrolyzed metal ions was not altered in the adsorption process (*36*). Thus, if we assume a 1:1 stoichiometry between Fe ions and surface silanol groups and that the adsorbed ions retain the same hydration sphere they had in solution, $\rho_{Fe,sorbed}$ was 100 ± 20 μm s^{-1} (Table 3). If adsorption results in the loss of one or two water molecules from the inner coordination sphere of the ion, then $\rho_{Fe,sorbed}$ could be as high as 160 ± 30 μm s^{-1}.

In comparison, $\rho_{Mn,sorbed}$ for Mn(II) ions at 4°C (*24*) was 100 times lower than $\rho_{Fe,sorbed}$ at 25°C (Table 3). Part of this discrepancy can be explained by an increase in the residence time of water molecules (τ_M) at a mineral surface with decreasing temperature; at low temperatures, the exchange of adsorbed water molecules with those in the pore fluid is slower. Also, T_{1M} (Eq. [6]) for adsorbed molecules should be sensitive to temperature variation because both the rotational component and the residence time component of τ_{c1} and τ_{c2} are inversely dependent on temperature and on their proximity to the surface.

ρ_{Fe} was approximately the same for adsorbed Fe(III) ions and surface Fe(III) in pseudobrookite (Table 3). If this relationship holds for all Fe(III)-bearing solids, the effect of solid-phase Fe(III) on NMR can be predicted from a single average ρ_{Fe}. $\rho_{Fe,sorbed}$ may also match $\rho_{Fe,solid}$ for amorphous Fe(III) oxyhydroxide, but the oxyhydroxide data are so widely scattered that a meaningful comparison is impossible.

CONCLUSIONS

This study has shown that surface relaxivity is constant for each pure mineral and that observed surface relaxivity parameters are weighted averages of these inherent relaxivities. Therefore, ρ can increase linearly from 10^{-3} to 10^{2} μm s^{-1} for solids with increasing surface concentrations of Fe(III). This variation is as great as the variation typically observed for pore size distribution in natural geological materials (*34*). We have also found that NMR relaxation measurements are so sensitive to paramagnetic impurities that most natural samples will probably have ρ values above 1 μm s^{-1}. For NMR of many rocks, iron concentrations are high enough that surface relaxivity could be considered to be relatively constant, but shifts in relaxation time distributions between samples should not automatically be attributed to shifts in pore size distribution unless it has been determined that paramagnetic content has not changed. For example, an interesting observation made by Hinedi *et al.* (*9*) when quantifying the microporosity of Borden Aquifer material was that the unfractionated material relaxed faster than the nonmagnetic fraction; they attributed the lower relaxation time to intraparticle microporosity of the iron oxide minerals. Because Fe(III)-bearing solid phases directly influence surface relaxivity, the lower relaxation times observed by Hinedi *et al.* (*9*) for the unfractionated material could be the result of higher ρ rather than smaller pores.

We have also shown that the ability of Fe(III) species at a surface to relax the NMR signal was greater than Fe(III) in solution and varies somewhat with the chemical state and location the Fe(III) material has. The increase in surface relaxivity observed for natural sand below pH 3 (*29*) can now be

explained by the dissolution of iron-bearing minerals and the subsequent adsorption of the Fe(III) ions to the quartz surface.

The concentration of Fe(III) in the pore fluid and at the solid surfaces can be calculated using geochemical software as long as information about pH, oxidation conditions, and mineralogy are known. Therefore, with mineral-specific ρ_{Fe} values, it should now be possible to predict ρ for a variety of natural systems containing iron(III) minerals, subsequently improving the accuracy of pore size calculations from relaxation time distributions. If the individual $\tau_M + T_{1M}$ (ρ_{Fe}) are not available for all possible minerals, one may be able to use average values to estimate ρ.

ACKNOWLEDGMENTS

This research was supported in full by funding to R.J.K. under Grant No. DE-FG07-96ER14711, Environmental Management Science Program, Office of Science and Technology, Office of Environment Management, U.S. Department of Energy (DOE). However, any opinions, findings, conclusions, or recommendations expressed herein are those of the authors and do not necessarily reflect the views of DOE. We thank Alex Mackay for the use of his NMR spectrometer and for valuable suggestions concerning experimental details. We also thank Frank Linseisen for his assistance with data processing and Joyce McBeth for her assistance with NMR measurements.

REFERENCES

1. R. J. S. Brown and B. W. Gamson, Nuclear magnetism logging, *Trans. Am. Inst. Min., Metall. Pet. Eng.* **219,** 199–207 (1960).
2. J. A. Jackson, Nuclear magnetic resonance well logging, *Log Analyst* **25,** 16–30 (1984).
3. G. C. Borgia and P. Fantazzini, Nonmobile water quantified in fully saturated porous materials by magnetic resonance relaxation and electrical resistivity measurements, *J. Appl. Phys.* **75,** 7562–7564 (1991).
4. M. G. Prammer, E. D. Drack, J. C. Bouton, and J. S. Gardner, Measurements of clay-bound water and total porosity by magnetic resonance logging, *Log Analyst* **37,** 61–69 (1996).
5. W. E. Kenyon, Petrophysical principles of applications of NMR logging, *Log Analyst* **38,** 21–43 (1997).
6. D. Chang, H. J. Vinegar, C. E. Morriss, and C. Straley, Effective porosity, producible field and permeability in carbonates from NMR logging, *Log Analyst* **38,** 60–72 (1997).
7. W. A. Kanters, R. J. Knight, and A. L. Mackay, Effects of wettability and fluid chemistry on the proton NMR T_1 in sands, *J. Environ. Eng. Geophys.* **3,** 197–202 (1998).
8. M. Schirov, A. Legchenko, and G. Creer, New direct non-invasive ground water detection technology for Australia, *Explor. Geophys.* **22,** 333–338 (1991).
9. Z. R. Hinedi, A. C. Chang, M. A. Anderson, and D. B. Borchardt, Quantification of microporosity by nuclear magnetic resonance relaxation of water imbibed in porous media, *Water Resour. Res.* **33,** 2697–2704 (1997).
10. H. G. Hertz, Nuclear magnetic relaxation spectroscopy, *in* "Water: A Comprehensive Treatise" (F. Franks, Ed.), Vol. 3, Chap. 7, Plenum, New York (1973).
11. K. F. Clark, *in* "Handbook of Physical Properties of Rocks" (R. S. Carmichael, Ed.), Vol. 1, Chap. 1, CRC Press, Boca Raton, FL (1982).
12. R. L. Kleinberg and H. J. Vinegar, NMR properties of reservoir fluids, *Log Analyst* **37,** 20–32 (1996).
13. J. R. Vogeley and C. O. Moses, ^{1}H NMR relaxation and rock permeability, *J. Colloid Interface Sci.* **56,** 2947–2953 (1992).
14. I. Foley, S. A. Farooqui, and R. L. Kleinberg, Effect of paramagnetic ions on NMR relaxation of fluids at solid surfaces, *J. Magn. Reson. A* **123,** 95–104 (1996).
15. J. J. Howard, W. E. Kenyon, and C. Straley, Proton magnetic resonance and pore size variations in reservoir sandstones, *SPE Form. Eval.* September, 194–200 (1993).
16. W. E. Kenyon and J. A. Kolleeny, NMR surface relaxivity of calcite with adsorbed Mn^{2+}, *J. Colloid Interface Sci.* **170,** 502–514 (1995).
17. S. D. Senturia and J. D. Robinson, Nuclear spin–lattice relaxation of liquids confined in porous solids, *Soc. Pet. Eng. J.* **10,** 237–244 (1970).
18. K. R. Brownstein and C. E. Tarr, Importance of classical diffusion in NMR studies of water in biological cells, *Phys. Rev. A* **19,** 2446–2453 (1979).
19. I. Solomon, Relaxation processes in a system of two spins, *Phys. Rev.* **99,** 559–565 (1955).
20. N. Bloembergen and L. O. Morgan, Proton relaxation times in paramagnetic solutions. Effects of electron spin relaxation, *J. Chem. Phys.* **34,** 842–850 (1961).
21. S. H. Koenig and R. D. Brown, *in* "Relaxometry of Paramagnetic Ions in Tissue: Metal Ions in Biological Systems" (H. Seigel, Ed.), p. 231, Dekker, New York (1987).
22. R. L. Kleinberg, W. E. Kenyon, and P. P. Mitra, Mechanism of NMR relaxation of fluids in rocks, *J. Magn. Reson. A* **108,** 206–214 (1994).
23. J. Korringa, D. O. Seevers, and H. C. Torrey, Theory of spin pumping and relaxation in systems with a low concentration of electron spin resonance centers, *Phys. Rev.* **127,** 1143–1150 (1962).
24. P. Roose, J. Van Craen, G. Andriessens, and H. Eisendrath, NMR study of spin–lattice relaxation of water protons by Mn^{2+} adsorbed onto colloidal silica, *J. Magn. Reson. A* **120,** 206–213 (1996).
25. M. C. Grantham, P. M. Dove, and T. J. DiChristina, Microbially catalyzed dissolution of iron and aluminum oxyhydroxide mineral surface coatings, *Geochim. Cosmochim. Acta* **61,** 4467–4477 (1997).
26. K. P. Whittall and A. L. Mackay, Quantitative interpretation of NMR relaxation data, *J. Magn. Reson.* **84,** 134–152 (1989).
27. K. P. Whittall, M. J. Bronskill, and R. M. Henkelman, Investigation of analysis techniques for complicated NMR relaxation data, *J. Magn. Reson.* **95,** 221–234 (1991).
28. T. S. Ramakrishnan, L. M. Schwartz, E. Fordham, W. E. Kenyon, and D. Wilkinson, Forward Models for Nuclear Magnetic Resonance in Carbonate Rocks, *Log Analyst* **40,** 260–270 (1999).
29. M. B. Caputi, Investigations of NMR T_1 relaxation mechanisms in oil- and water-wet sand packs, M.Sc. dissertation, Univ. of British Columbia, Vancouver, BC, Canada, 1997.
30. J. H. Simpson and H. Y. Carr, Diffusion and nuclear spin relaxation in water, *Phys. Rev.* **111,** 1201–1202 (1958).
31. D. O. Seevers, A nuclear magnetic method for determining the permeability of sandstones, *SPWLA 7th Annu. Logging Symp. Proc.,* paper L (1966).
32. L. L. Latour, R. L. Kleinberg, and A. Sezginer, Nuclear magnetic resonance properties of rocks at elevated temperatures, *J. Colloid Interface Sci.* **150,** 535–548 (1992).
33. I. Bertini, F. Capozzi, C. Luchinat, and Z. Xia, Nuclear and electron relaxation of $Fe(OH_2)_6^{3+}$, *J. Phys. Chem.* **97,** 1134–1137 (1993).

34. S. P. Roberts, P. J. Macdonald, and T. Tritchard, A bulk and spatially resolved NMR relaxation study of sandstone rock plugs, *J. Magn. Reson. A* **116,** 189–195 (1995).

35. P. W. Schindler, B. Fürst, R. Dick, and P. U. Wolf, Ligand properties of surface silanol groups. 1. Surface complex formation with Fe^{3+}, Cu^{2+}, Cd^{2+}, and Pb^{2+}, *J. Colloid Interface Sci.* **55,** 469–475 (1976).

36. R. O. James and T. W. Healy, Adsorption of hydrolyzable metal ions at the oxide–water interface, *J. Colloid Interface Sci.* **40,** 42–81 (1972).

37. F. D'Orazio, J. C. Tarczon, W. P. Halperin, K. Eguchi, and T. Mizusaki, Application of nuclear magnetic resonance pore structure analysis to porous silica glass, *J. Appl. Phys.* **65,** 742–750 (1989).

38. D. P. Gallegos, D. M. Smith, and C. J. Brinker, An NMR technique for the analysis of pore structure: Application to mesopores and micropores, *J. Colloid Interface Sci.* **124,** 186–189 (1988).

39. D. Langmuir, *in* "Aqueous environmental geochemistry," p. 432, Prentice-Hall, Upper Saddle River, NJ (1997).